Polarization physics at the high p_T region on the JINT LHE acceleration complex

S.S. Shimanskiy (JINR,Dubna)

Plan

1. Why so important the high p_T physics in energy range up to $\sqrt{s_{NN}} \sim 10GeV$?

2. Polarization studies with polarized ion beams.

3. *pp (at 90° c.m.s.) and cumulative physics with polarized beams.*

Why so important the high pT physics in energy up to $\sqrt{s_{NN}} \sim 10GeV$?

RHIC Physics: 3 Lectures*

Larry McLerran

Physics Department PO Box 5000 Brookhaven National Laboratory Upton, NY 11973 USA

September 13, 2003

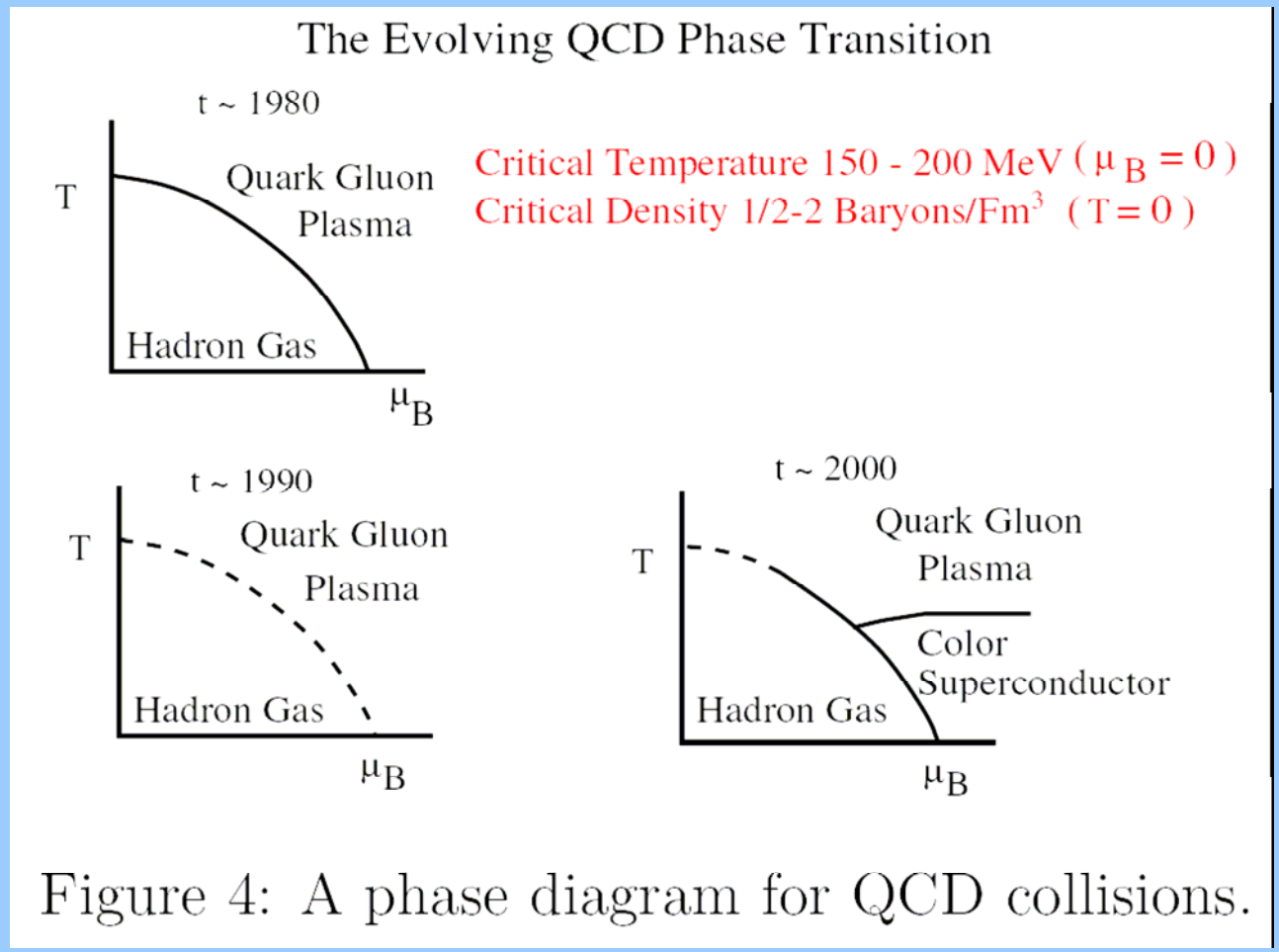

Figure 4: A phase diagram for QCD collisions.

QCD phase diagram

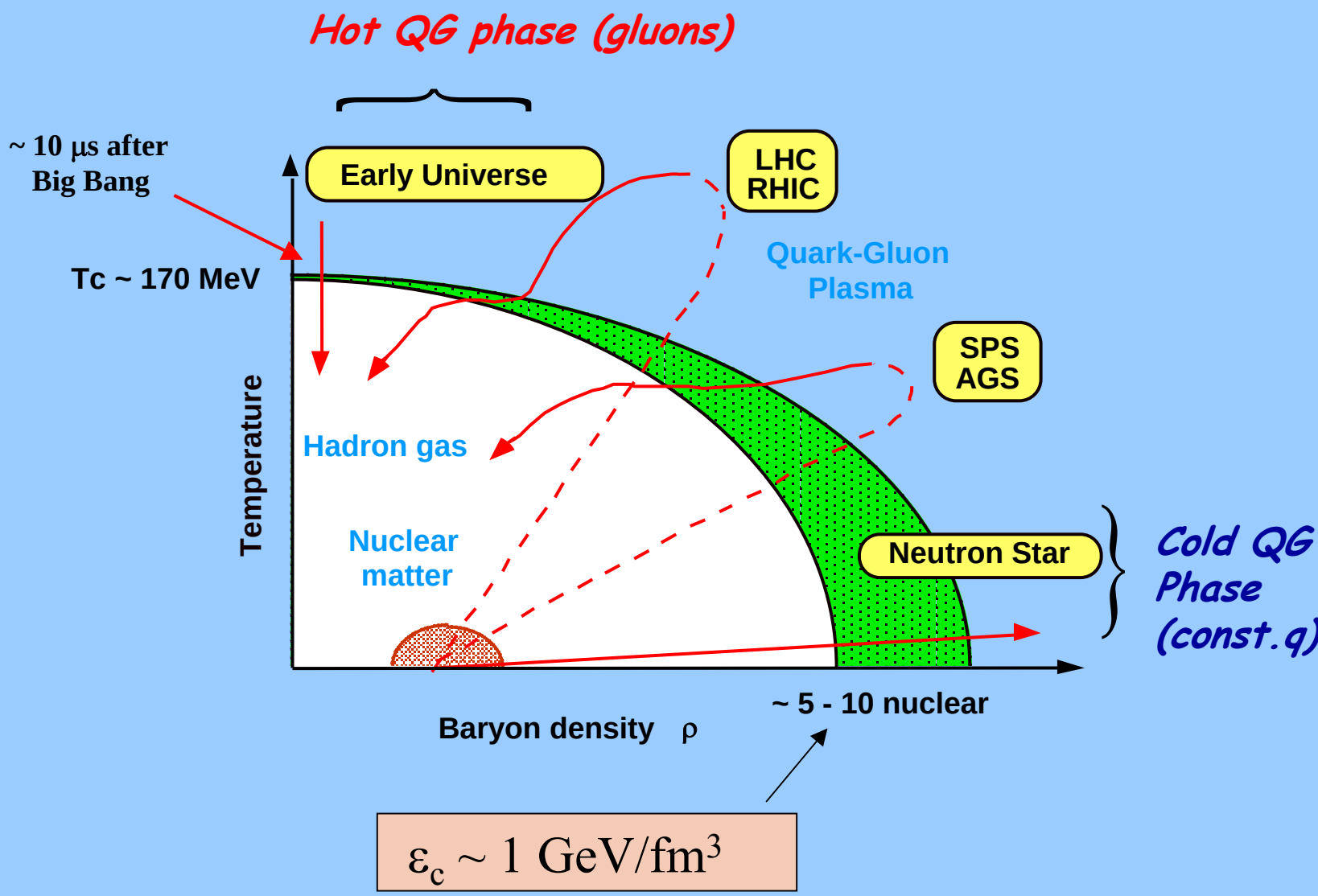

What if we compress/heat the system so much that the individual hadrons start to interpenetrate?

II.Way for Hot QG phase

Heavy AA-collisions

1. QGP, sQGP, CGC, GLAZMA or …
2. Early time of Universe evolution

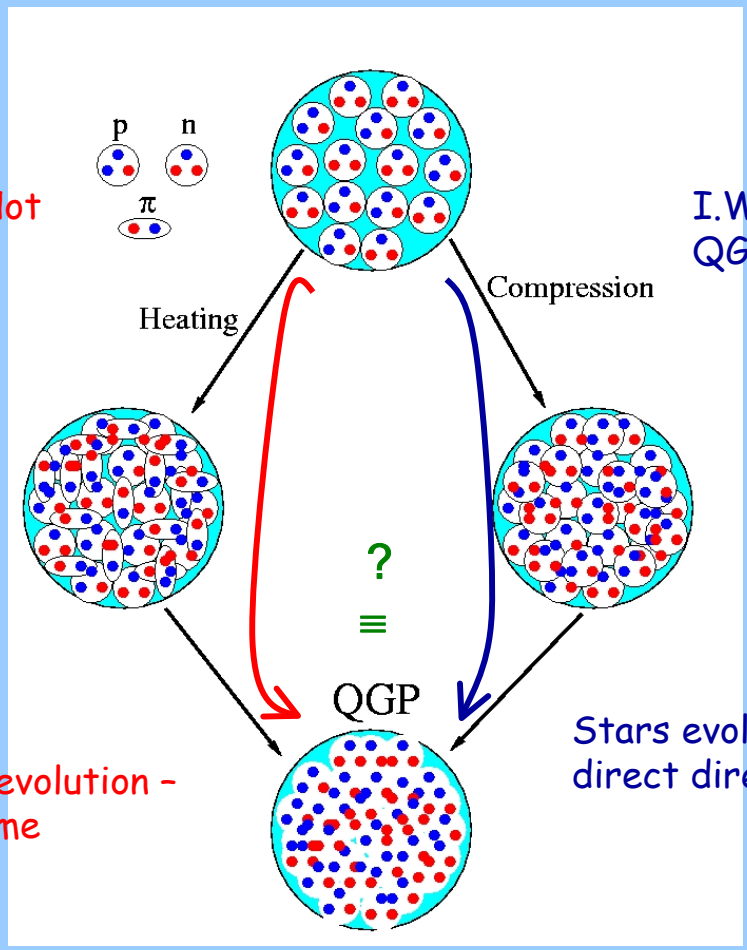

I.Way for Cold QG phase

Cumulative and high p_T physics

1. Multiquarks states in the cold nuclear matter or …
2. Properties of the multiquarks states, high density states
3. Stars evolution, dark matter

Universe evolution – back in time

Stars evolution - direct direction

Final phases will be equal or not?

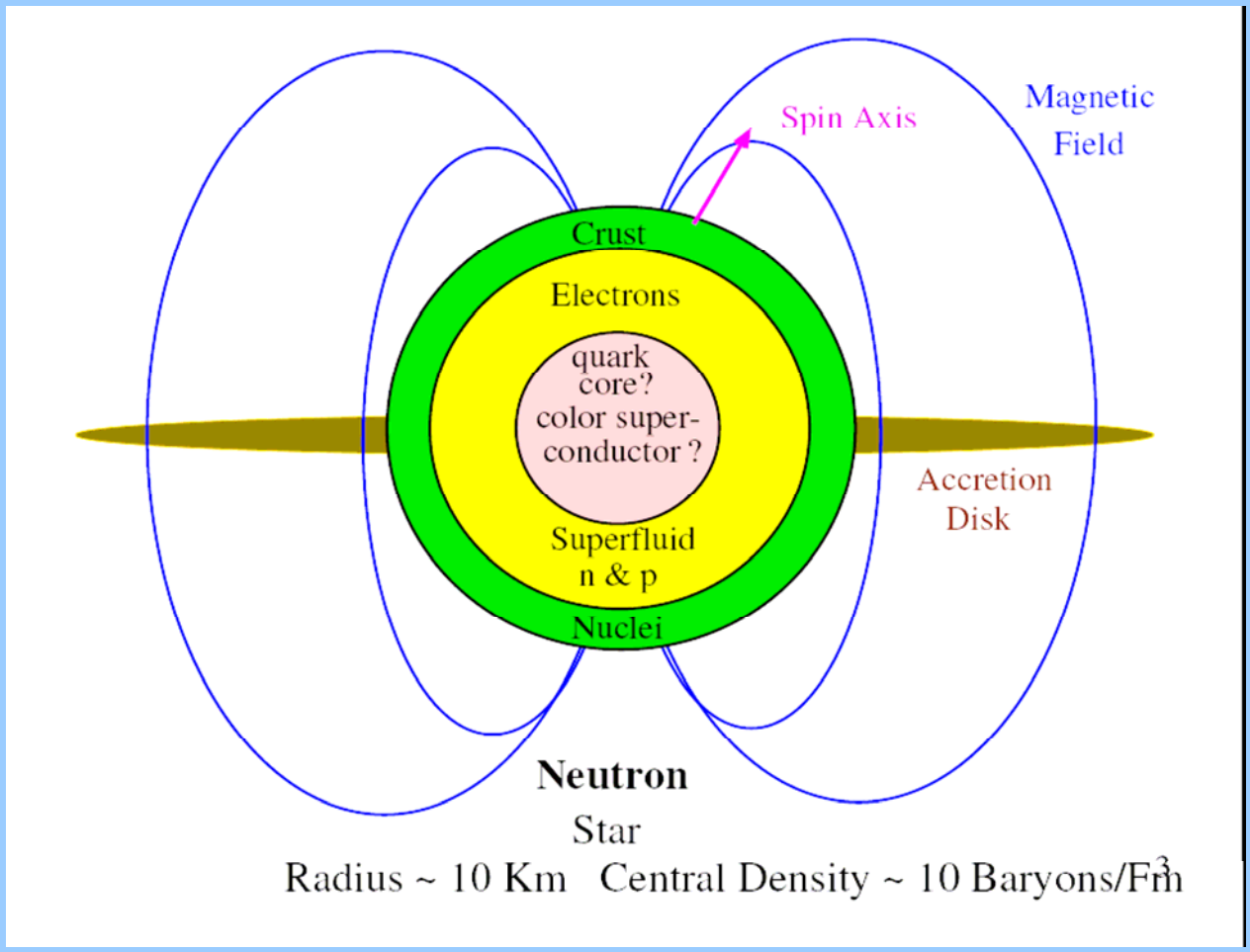

A spinning neutron star

Stars can have magnetic fields ~ 10^{18} Gs

K.Rith From Nuclei to Nucleons (Summary)
Nuclear Physics A532 (1991) 3c-14c

2.6. Region 5

In the region $x > 1$ the struck quark is 'superfast', its momentum is larger than the momentum allowed for a stationary nucleon. The longitudinal distances involved are $z < 0.2$ fm and therefore one is sensitive to correlations of nearby nucleons or more complicated configurations like multiquark clusters. As an example the predictions for a multiquark cluster calculation [32] are shown in figure 5.

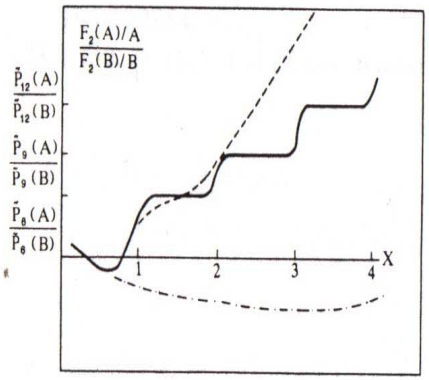

Figure 5. Theoretical predictions for nuclear structure functions at $x > 1$

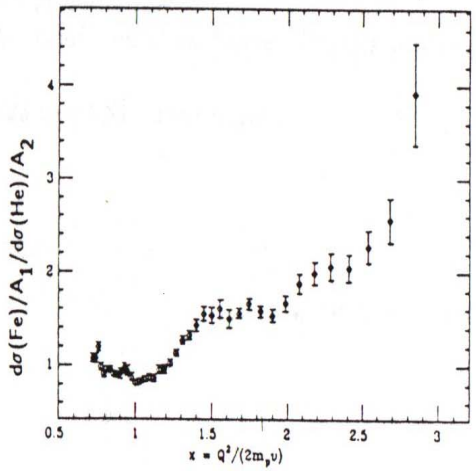

Figure 6. Preliminary results for σ^{Fe}/σ^{He} from NE-2 at SLAC

The height of the plateau in the range $1 < x < 2$ is proportional to the ratio of probabilities of finding 6-quark clusters in nuclei A and B, the range $2 < x < 3$ reflects the ratio of 9-quark cluster probabilities and so on.

Figure 6 shows preliminary results for the cross section ratio of Fe and He obtained by NE-2 at SLAC [33], which took data for a series of nuclei with beam energies between 4 and 14 GeV. One could speculate that the plateau for $1.5 < x < 2$ is an indication for the step function expected in the multiquark cluster model. Note, however, that the data are still substantially affected by quasielastic scattering as the ratio is smaller than one near $x = 1$.

32 J. Vary, Proceedings of the 7th Int. Conf. on High Energy Physics problems, Dubna 1984,147.

nucl-ex/0508026

Measurement of 2- and 3-Nucleon Short Range Correlation Probabilities in Nuclei

K.S. Egiyan,[1] N.B. Dashyan,[1] M.M. Sargsian,[10] M.I. Strikman,[28] L.B. Weinstein,[27] G. Adams,[30] P. Ambrozewicz,[10] M. Anghinolfi,[16] B. Asavapibhop,[22] G. Asryan,[1] H. Avakian,[34] H. Baghdasaryan,[27] N. Baillie,[38] J.P. Ball,[2]

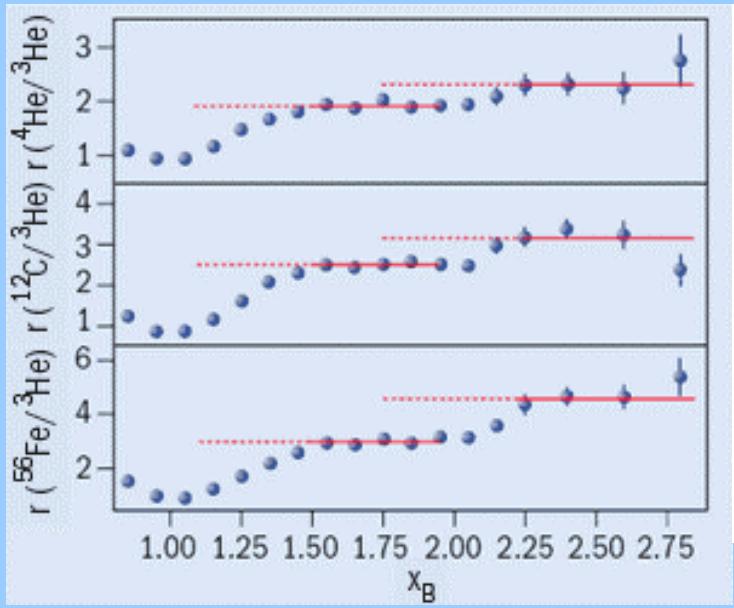

$$r(A,{}^3\mathrm{He}) = \frac{A(2\sigma_{ep}+\sigma_{en})}{3(Z\sigma_{ep}+N\sigma_{en})}\frac{3\mathcal{Y}(A)}{A\mathcal{Y}({}^3\mathrm{He})}C^A_{\mathrm{rad}}, \qquad (2)$$

where Z and N are the number of protons and neutrons in nucleus A, σ_{eN} is the electron-nucleon cross section, $\mathcal{Y}$ is the normalized yield in a given (Q^2,x_B) bin [30] and C^A_{rad} is the ratio of the radiative correction factors for A and ^{3}He ($C^A_{\mathrm{rad}} = 0.95$ and 0.92 for ^{12}C and ^{56}Fe respectively). In our Q^2 range, the elementary cross section correction factor $\frac{A(2\sigma_{ep}+\sigma_{en})}{3(Z\sigma_{ep}+N\sigma_{en})}$ is 1.14 ± 0.02 for C and ^{4}He and 1.18 ± 0.02 for ^{56}Fe. Fig. 1 shows the resulting ratios integrated over $1.4 < Q^2 < 2.6$ GeV^2.

Polarization studies with polarized ion beams.

Need to help us in finding of answers for:

1. Do we really see multiquark states in nuclear mater (diquark in a proton)?

2. How are constituents interact (not as predicted by pQCD)?

JINR

Veksler & Baldin Laboratory of High Energies

Dubna

NUCLOTRON

Beams	Intensity (particles per cycle)	
	available now	next step
p	$2.5 \cdot 10^{10}$	10^{13}
d	$5 \cdot 10^{10}$	10^{13}
d↑	$3 \cdot 10^{8}$	$5 \cdot 10^{10}$
^{4}He	$8 \cdot 10^{8}$	$2 \cdot 10^{12}$
^{7}Li	$2 \cdot 10^{9}$	$5 \cdot 10^{12}$
^{10}B	$2 \cdot 10^{7}$	10^{10}
^{12}C	$6.5 \cdot 10^{8}$	$2 \cdot 10^{12}$
^{24}Mg	$1.2 \cdot 10^{8}$	$5 \cdot 10^{11}$
^{40}Ar	10^{8}	10^{10}
^{56}Fe	10^{6}	10^{11}
^{84}Kr	10^{3}	$5 \cdot 10^{8}$

Nuclotron-M, NICA and polarized ion beams

"The possibility to accelerate a Polarized Beam of p, d, t, ^{3}He at JINR nuclotron"

Presented by Yuri Filatov at DSPIN07 05.09.2007

Polarized ion source based on CIPIOS(IUCF)

How we can define constituents?

Quark counting rules

In 1973 were published two artiles :

Matveev V.A., Muradyan R.M., Tavkhelidze A.N. Lett. Nuovo Cimento ***7****,719 (1973);*

Brodsky S., Farrar G. Phys. Rev. Lett. ***31****,1153 (1973)*

Predictions that for momentum $p_{beam} \geq 5$ GeV/c in any binary large-angle scattering ($\theta_{cm} > 40^{o}$) reaction at large momentum transfers $Q = \sqrt{-t}$:

A + B -> C + D

$$\frac{d\sigma}{dt}_{A+B->C+D} \sim s^{-(n_A+n_B+n_C+n_D-2)} f(\frac{t}{s})$$

where n_A, n_B, n_C and n_D the amounts of elementary constituents in A, B, C and D.

$s=(p_A+p_B)^2$ и $t=(p_A-p_C)^2$,

$$\frac{d\sigma}{dt}_{pp->pp} \sim s^{-10} \quad \text{and} \quad \frac{d\sigma}{dt}_{\pi p -> \pi p} \sim s^{-8}$$

Soft Perturbative QCD*

Paul Hoyer

NORDITA-1999/52 HE
hep-ph/9908501
August 30, 1999

The way the differential large angle $2 \to 2$ particle scattering cross sections should scale with energy (momentum transfer) was envisaged by the so-called "quark counting rules" [26].

$$\frac{d\sigma}{dt} = \frac{f(\Theta)}{s^{K-2}}; \qquad \frac{t}{s} = \text{const},$$

with K the number of *elementary fields* (quarks, photons, leptons, etc.) among / inside the initial and final particles.

For example, in the case of the deuteron break-up by a photon, $\gamma + D \to p + n$, we have $K = 1 + 6 + 6 = 13$ (a photon and 6 quarks inside the initial deuteron and another 6 in the final proton and neutron). So, the differential cross section is expected to fall with s, *asymptotically*, as $s^{-11} = E_{\text{c.m.}}^{-22}$.

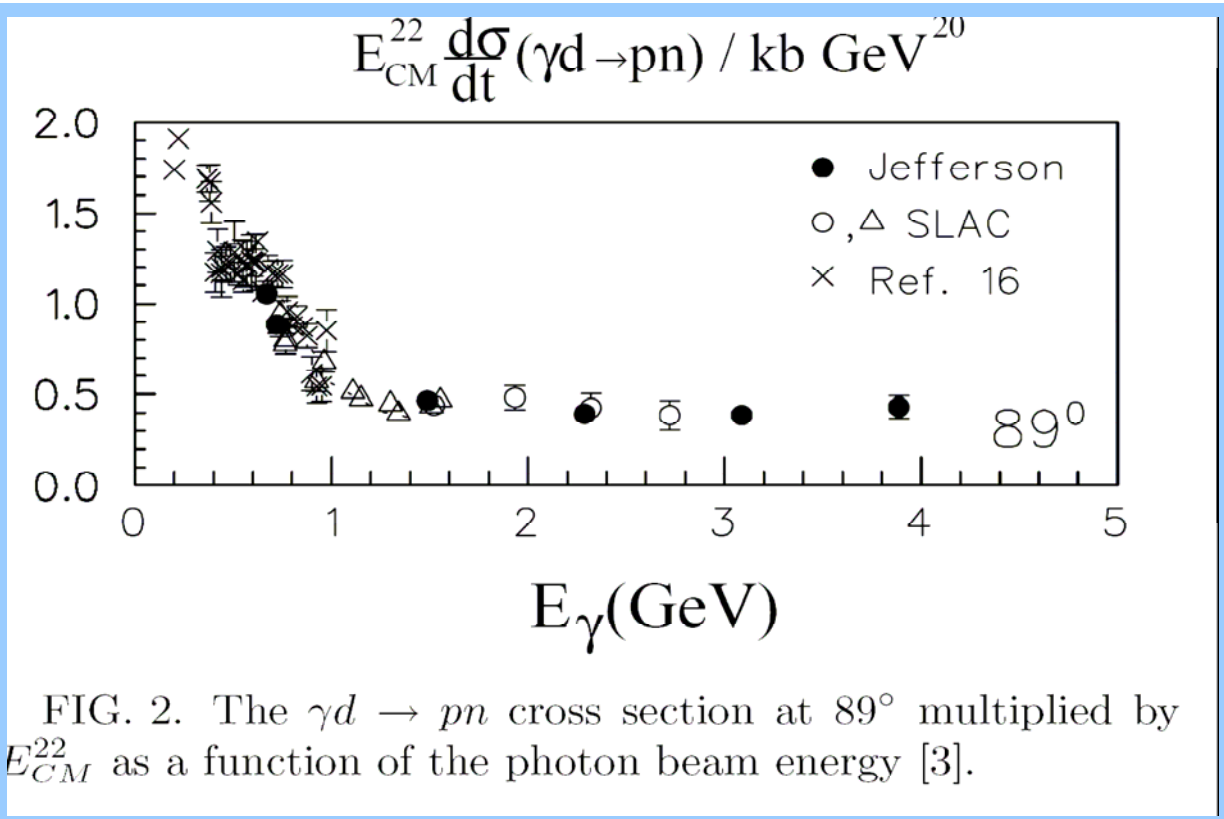

FIG. 2. The $\gamma d \to pn$ cross section at 89° multiplied by E_{CM}^{22} as a function of the photon beam energy [3].

Eur. Phys. J. A 8, 423–428 (2000)

The cross-section asymmetry Σ is determined using the reaction yield $N_n \rightarrow$ and $N_n \uparrow$ for photon polarization parallel and perpendicular to the reaction plane:

$$\Sigma = (N_n \rightarrow - N_n \uparrow)/(\bar{P}_\gamma \uparrow N_n \rightarrow + \bar{P}_\gamma \rightarrow N_n \uparrow), \quad (1)$$

where $\bar{P}_\gamma \uparrow$, $(\bar{P}_\gamma \rightarrow)$ is the mean value of the photon polarization in the E_γ acceptance.

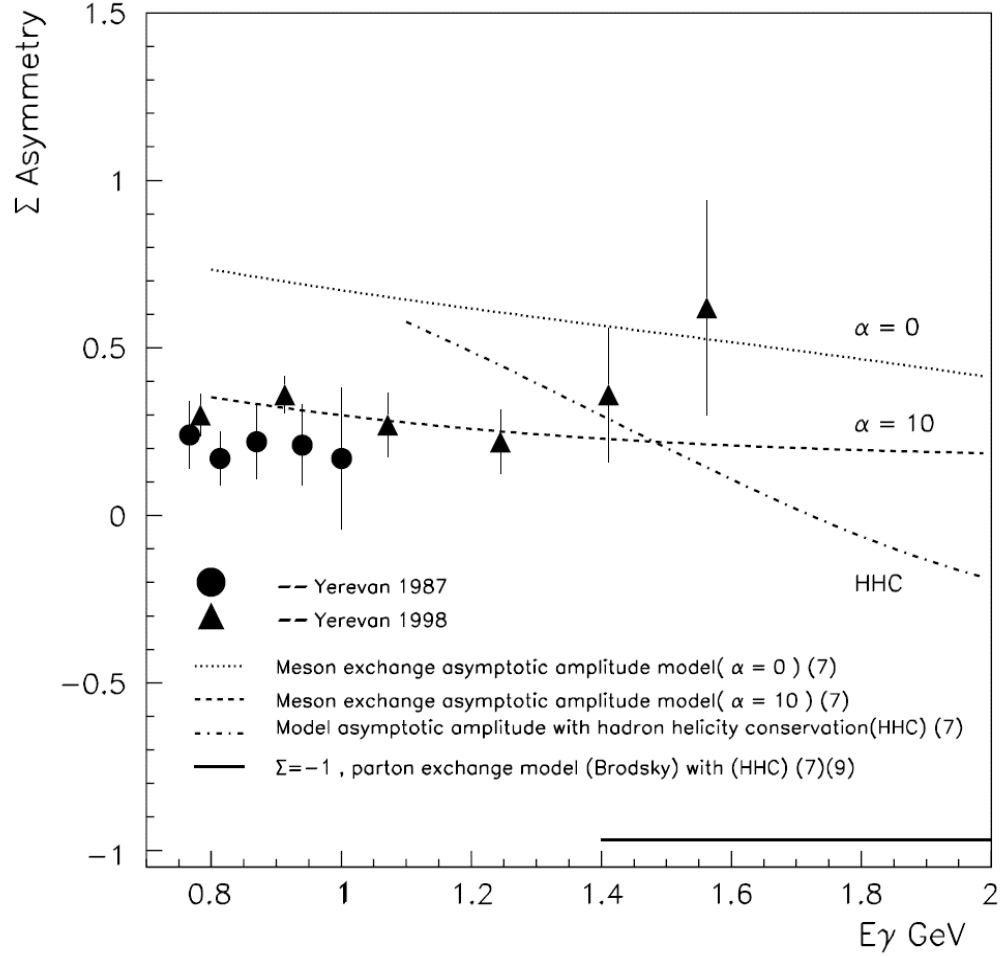

Fig. 8. The energy dependence of the cross-section asymmetry Σ for $\theta_p = 90^\circ$ in the cms.

nucl-th/0307032 v1 9 Jul 2003

Forward-backward angle asymmetry and polarization observables in high-energy deuteron photodisintegration

V.Yu. Grishina [a], L.A. Kondratyuk [b], W. Cassing [c], E. De Sanctis [d], M. Mirazita [d], F. Ronchetti [d] and P. Rossi [d]

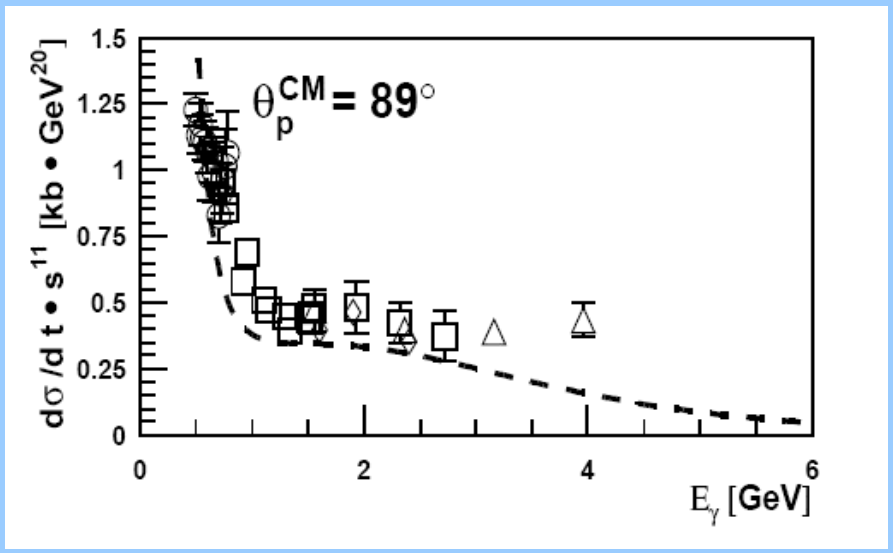

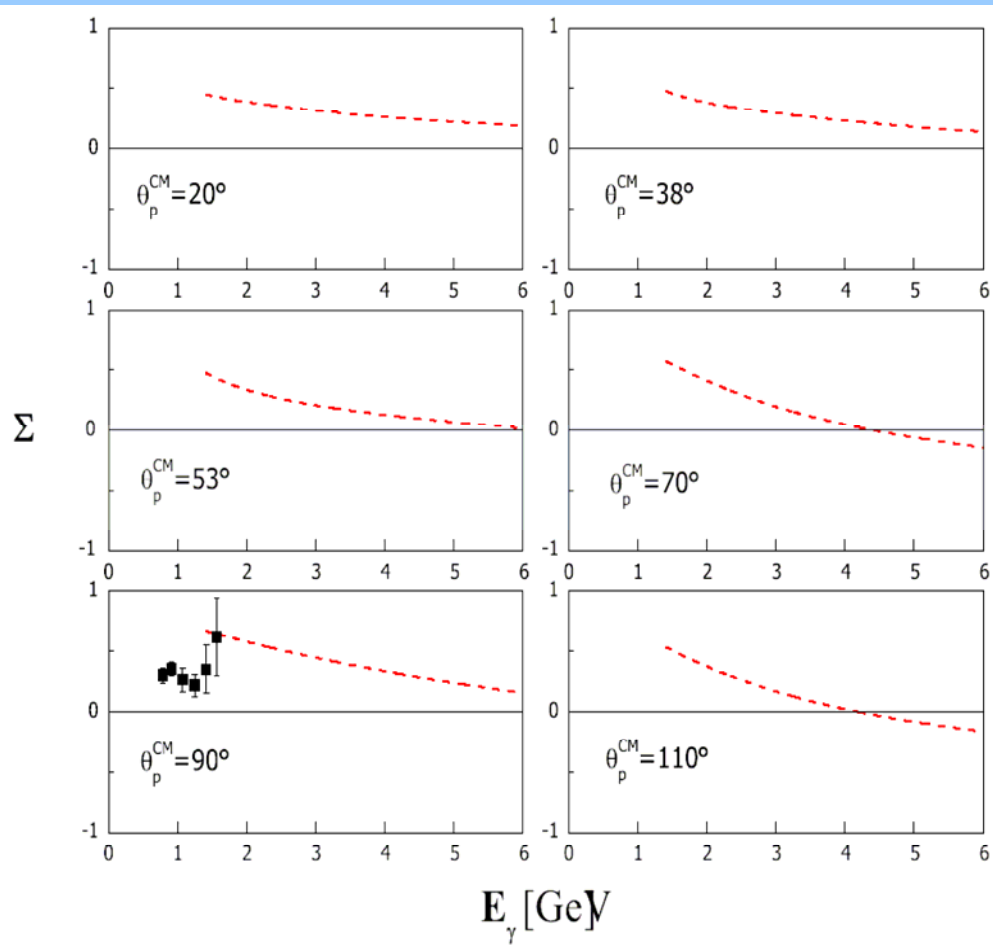

Pis'ma v ZhETF, vol. 81, iss. 7, pp. 387 – 390 © 2005 April 10

Indication of asymptotic scaling in the reactions $dd \to p^3\mathrm{H}$, $dd \to n^3\mathrm{He}$ and $pd \to pd$

Yu. N. Uzikov[1)]
Joint Institute for Nuclear Research, LNP, 141980 Dubna, Moscow region, Russia

Submitted 11 January 2005
Resubmitted 28 February 2005

It is shown that the differential cross sections of the reactions $dd \to n^3\mathrm{He}$ and $dd \to p^3\mathrm{H}$ measured at c.m.s. scattering angle $\theta_{cm} = 60^\circ$ in the interval of the deuteron beam energy 0.5–1.2 GeV demonstrate the scaling behaviour, $d\sigma/dt \sim s^{-22}$, which follows from constituent quark counting rules. It is found also that the differential cross section of the elastic $dp \to dp$ scattering at $\theta_{cm} = 125—135^\circ$ follows the scaling regime $\sim s^{-16}$ at beam energies 0.5–5 GeV. These data are parameterized here using the Reggeon exchange.

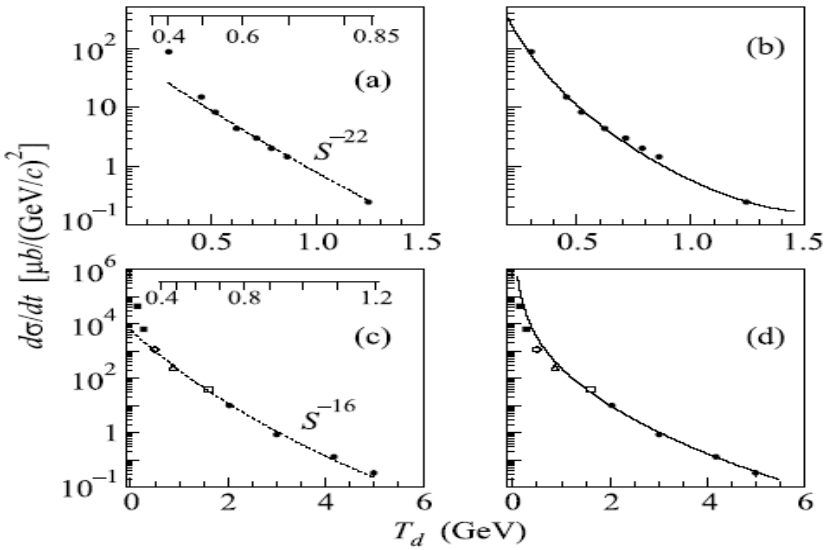

Fig.2. The differential cross section of the $dd \to n^3\mathrm{He}$ and $dd \to p^3\mathrm{H}$ reactions at $\theta_{cm} = 60^o$ (a), (b) and $dp \to dp$ at $\theta_{cm} = 127^o$ (c), (d) versus the deuteron beam kinetic energy. Experimental data in (a), (b) are taken from [20]. In (c), (d), the experimental data (black squares),(○), (△), (open square) and (●) are taken from [22 – 26], respectively. The dashed curves give the s^{-22} (a) and s^{-16} (c) behaviour. The full curves show the result of calculations using Regge formalism given by Eqs. (2), (3), (4) with the following parameters: (b) – $C_1 = 1.9\,\mathrm{GeV}^2$, $R_1^2 = 0.2\,\mathrm{GeV}^{-2}$, $C_2 = 3.5$, $R_2^2 = -0.1\,\mathrm{GeV}^{-2}$; (d) – $C_1 = 7.2\,\mathrm{GeV}^2$, $R_1^2 = 0.5\,\mathrm{GeV}^{-2}$, $C_2 = 1.8$, $R_2^2 = -0.1\,\mathrm{GeV}^{-2}$. The upper scales in (a) and (c) show the relative momentum q_{pn} (GeV/c) in the deuteron for the ONE mechanism

pp (at 90o c.m.s.) and cumulative physics with polarized beams.

SLAC – PUB – 4749
October 1988
(M)

ANTIPROTON ANNIHILATION IN QUANTUM CHROMODYNAMICS*

STANLEY J. BRODSKY

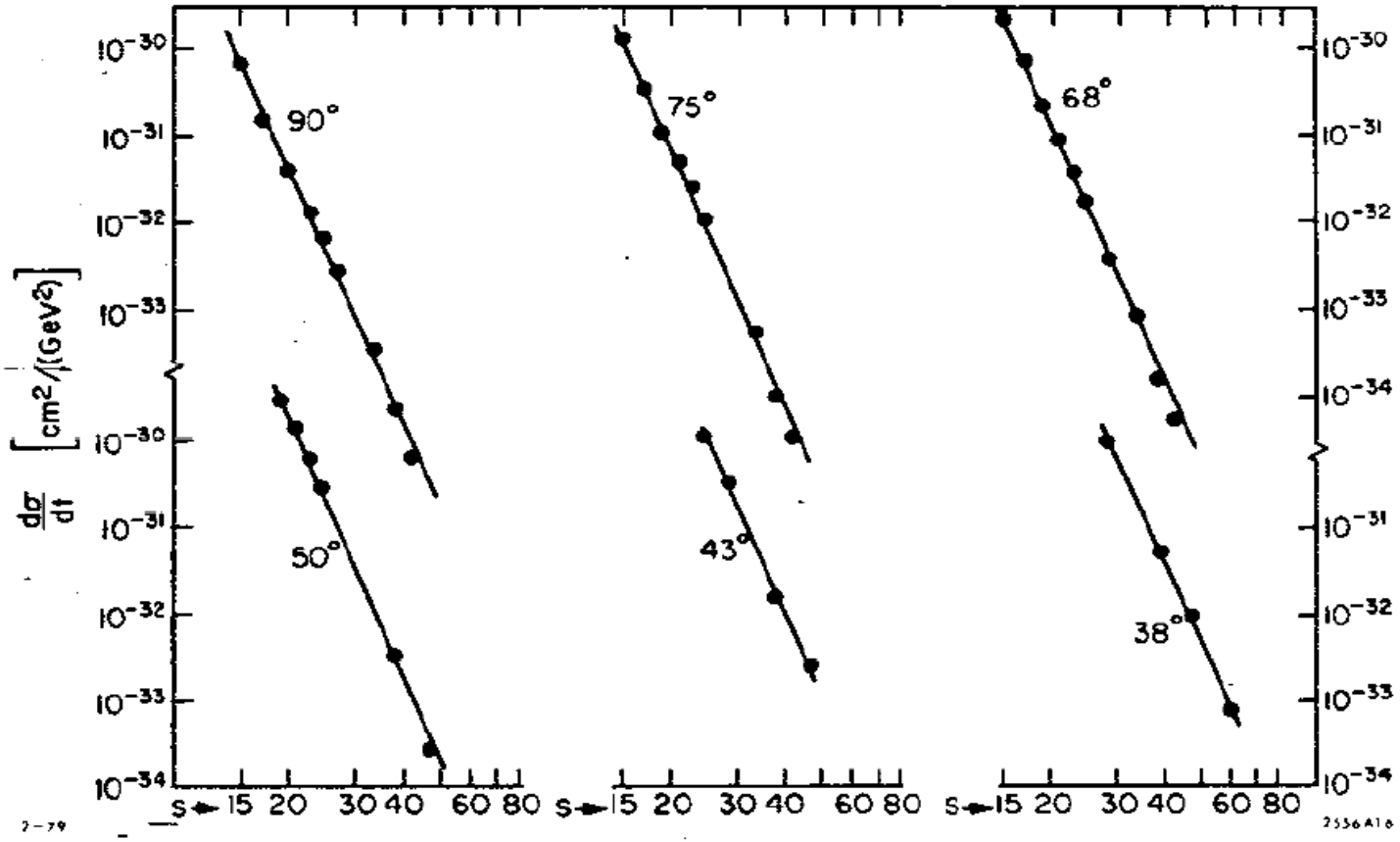

Fig. 16. Test of fixed θ_{CM} scaling for elastic pp scattering. The best fit gives the power $N = 9.7 \pm 0.5$ compared to the dimensional counting prediction N=10. Small deviations are not readily apparent on this log-log plot. The compilation is from Landshoff and Polkinghorne.

8 GeV/c

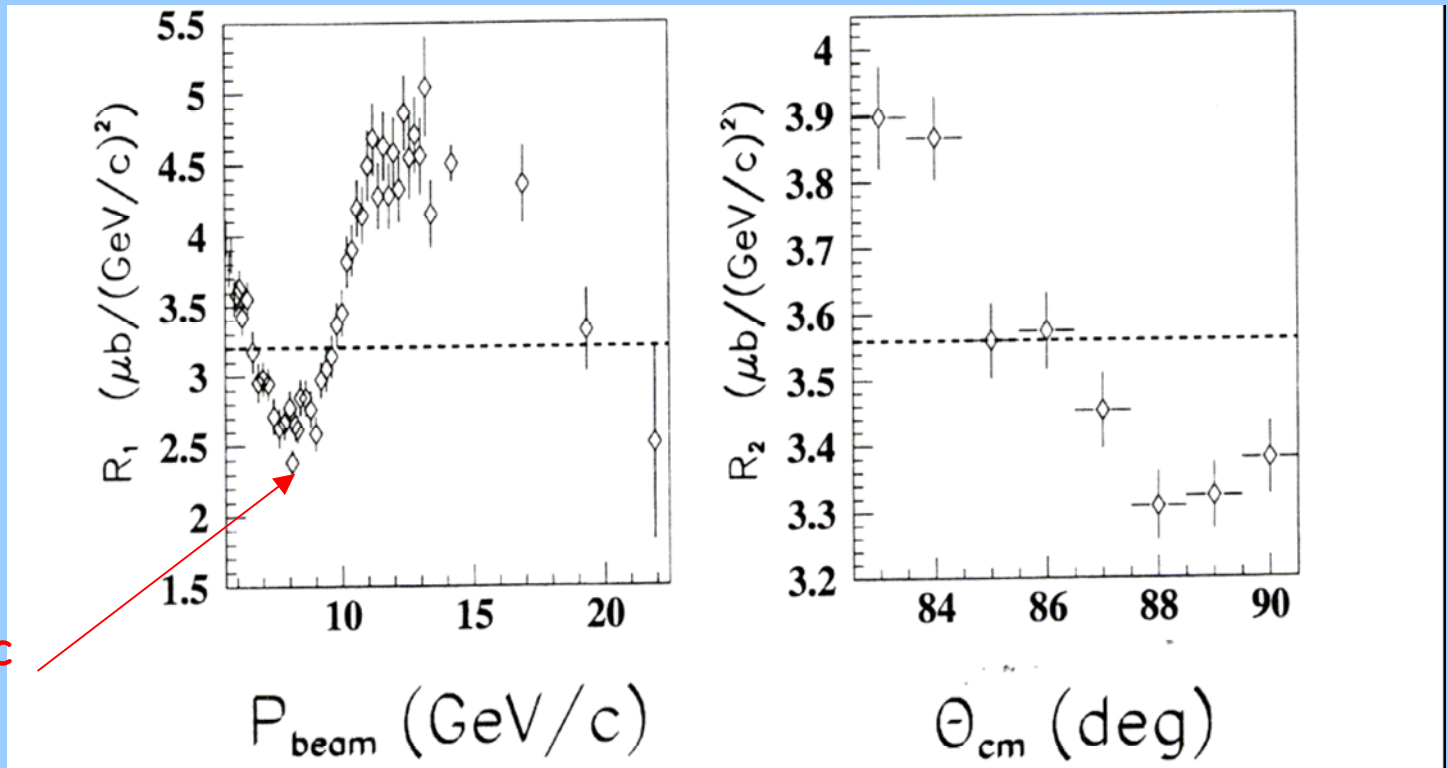

Figure 1.2: Scaled $pp \to pp$ differential cross sections. The dashed lines represent perfect scaling. Their vertical position is arbitrary. **Left** - $R_1 = (\left(\frac{s}{s_0}\right)^{10} \frac{d\sigma}{dt}(pp))^{-1}$ ($s_0 = 13\ GeV^2$) at $\theta_{cm} = 90^0$ versus incoming momentum. Data are from Ref. [19]. **Right** - $R_2 = (1 - \cos^2\theta_{cm})^{4\gamma} \frac{d\sigma}{dt}(pp)$ ($\gamma = 1.6$) at $p_{lab} = 5.9$ GeV/c versus θ_{cm}. Data are from Ref. [17].

PHYSICAL REVIEW D VOLUME 23, NUMBER 3 1 FEBRUARY 1981

Energy dependence of spin-spin effects in p-p elastic scattering at 90°$_{c.m.}$

E. A. Crosbie, L. G. Ratner, and P. F. Schultz
Argonne National Laboratory, Argonne, Illinois 60439

J. R. O'Fallon
Argonne Universities Association, Argonne, Illinois 60439

D. G. Crabb, R. C. Fernow,* P. H. Hansen,† A. D. Krisch, A. J. Salthouse,‡ B. Sandler,§ T. Shima, and K. M. Terwilliger
Randall Laboratory of Physics, The University of Michigan, Ann Arbor, Michigan 48109

N. L. Karmakar
University of Kiel, Kiel, Germany

S. L. Linn‖ and A. Perlmutter
Department of Physics and Center for Theoretical Studies, The University of Miami, Coral Gables, Florida 33124

P. Kyberd
Nuclear Physics Laboratory, Oxford University, Oxford, England
(Received 31 March 1980)

The energy dependence of the spin-parallel and spin-antiparallel cross sections for $p_\uparrow + p_\uparrow \to p + p$ at 90°$_{c.m.}$ was measured for beam momenta between 6 and 12.75 GeV/c. The ratio $(d\sigma/dt)_{\text{parallel}}:(d\sigma/dt)_{\text{antiparallel}}$ at 90° is about 1.2 up to 8 GeV/c and then increases rapidly to a value of almost 4 near 11 GeV/c. Our data indicate that this ratio may depend only on the variable $P_\perp{}^2$, and suggests that the ratio may reach a limiting value of about 4 for large $P_\perp{}^2$.

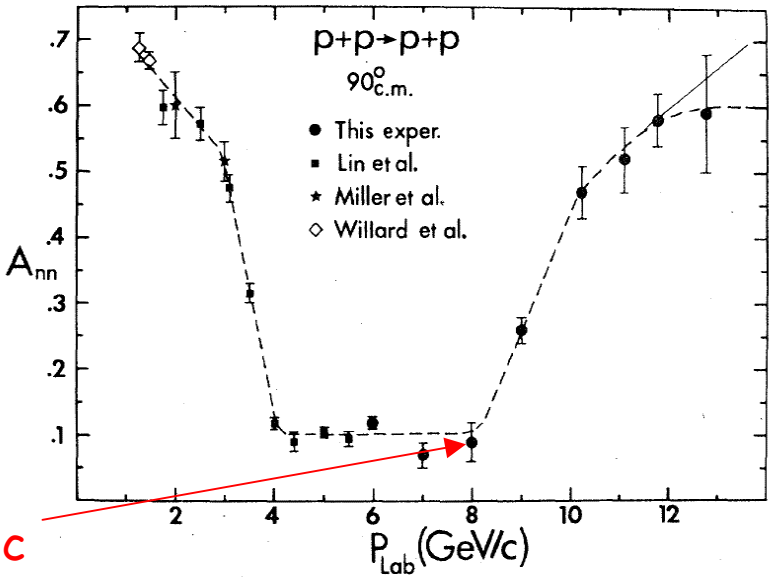

8 GeV/c

FIG. 2. Plot of the spin-spin correlation parameter A_{nn} for $p+p \to p+p$ at 90°$_{c.m.}$ as a function of incident beam momentum. The dashed and solid lines are hand-drawn possible fits.

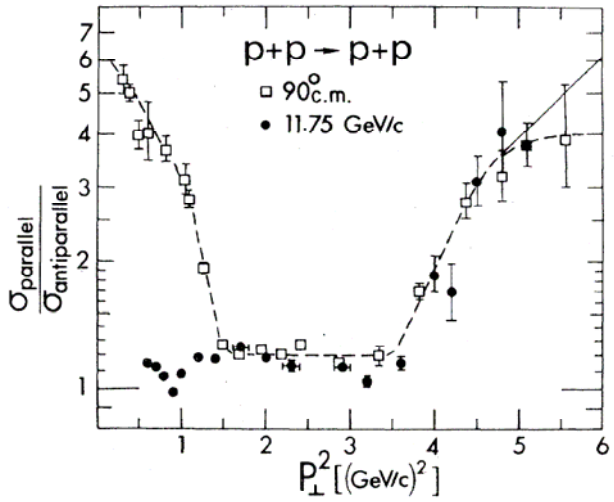

FIG. 3. Plot of the ratio of the spin-parallel to spin-antiparallel differential cross sections, as a function of $P_\perp{}^2$, for p-p elastic scattering. The squares are the fixed-angle data at 90°$_{c.m.}$, with the incident energy varied. The circles are data (Refs. 5, 11) with the momentum held fixed at 11.75 GeV/c while the scattering angle is varied. The dashed and solid lines are hand-drawn possible fits to the 90°$_{c.m.}$ data.

S.S.Shimanskiy

Color(nuclear) transparency in 90^0 c.m. quasielastic $A(p,2p)$ reactions

The incident momenta varied from 5.9 to 14.4 GeV/c, corresponding to $4.8 < Q^2 < 12.7$ (GeV/c)^2.

$$T = \frac{\frac{d\sigma}{dt}(p + \text{"}p\text{"} \rightarrow p + p)}{Z\frac{d\sigma}{dt}(p + p \rightarrow p + p)}$$

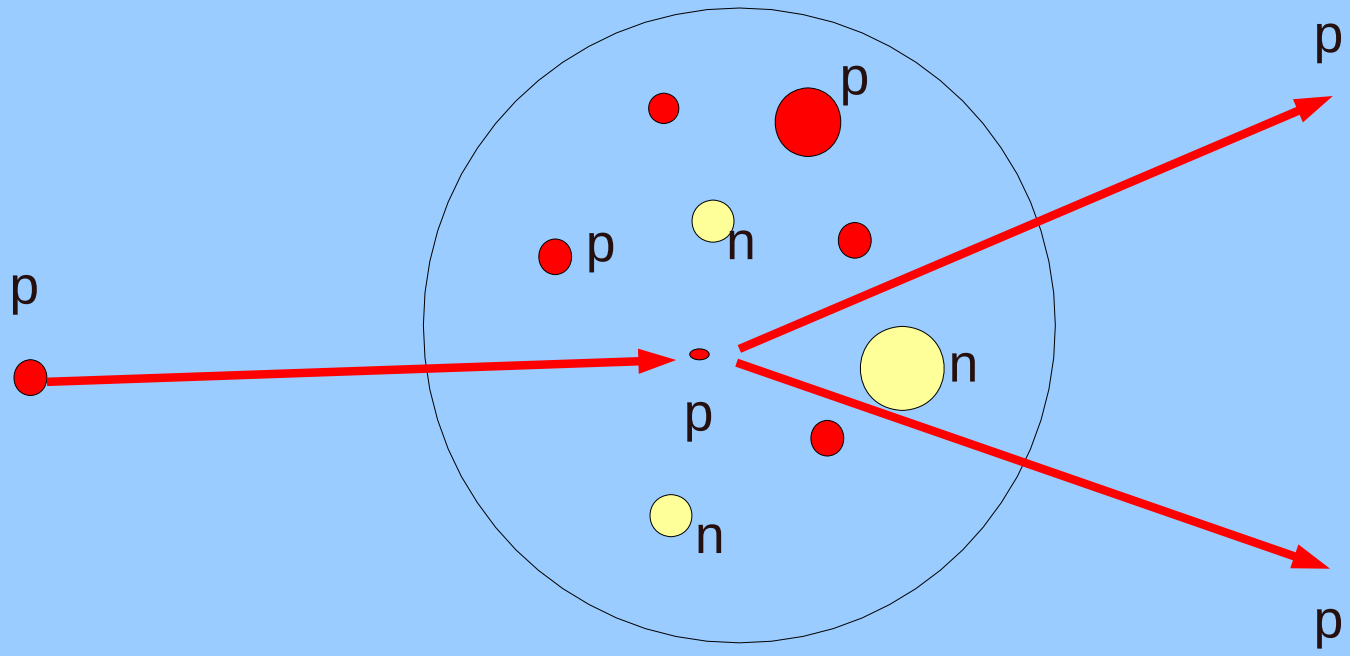

VOLUME 87, NUMBER 21 PHYSICAL REVIEW LETTERS 19 NOVEMBER 2001

Energy Dependence of Nuclear Transparency in C(p,2p) Scattering

A. Leksanov,[5] J. Alster,[1] G. Asryan,[3,2] Y. Averichev,[8] D. Barton,[3] V. Baturin,[5,4] N. Bukhtoyarova,[3,4] A. Carroll,[3] S. Heppelmann,[5] T. Kawabata,[6] Y. Makdisi,[3] A. Malki,[1] E. Minina,[5] I. Navon,[1] H. Nicholson,[7] A. Ogawa,[5] Yu. Panebratsev,[8] E. Piasetzky,[1] A. Schetkovsky,[5,4] S. Shimanskiy,[8] A. Tang,[9] J. W. Watson,[9] H. Yoshida,[6] and D. Zhalov[5]

[1]*School of Physics and Astronomy, Sackler Faculty of Exact Sciences, Tel Aviv University, Ramat Aviv 69978, Isra*
[2]*Yerevan Physics Institute, Yerevan 375036, Armenia*
[3]*Collider-Accelerator Department, Brookhaven National Laboratory, Upton, New York, 11973*
[4]*Petersburg Nuclear Physics Institute, Gatchina, St. Petersburg 188350, Russia*
[5]*Physics Department, Pennsylvania State University, University Park, Pennsylvania 16801*
[6]*Department of Physics, Kyoto University, Sakyoku, Kyoto, 606-8502, Japan*
[7]*Department of Physics, Mount Holyoke College, South Hadley, Massachusetts 01075*
[8]*J.I.N.R., Dubna, Moscow 141980, Russia*
[9]*Department of Physics, Kent State University, Kent, Ohio 44242*
(Received 20 April 2001; published 6 November 2001)

The transparency of carbon for (p, 2p) quasielastic events was measured at beam momenta ranging from 5.9 to 14.5 GeV/c at 90° c.m. The four-momentum transfer squared (Q^2) ranged from 4.7 to 12.7 (GeV/c)^2. We present the observed beam momentum dependence of the ratio of the carbon to hydrogen cross sections. We also apply a model for the nuclear momentum distribution of carbon to obtain the nuclear transparency. We find a sharp rise in transparency as the beam momentum is increased to 9 GeV/c and a reduction to approximately the Glauber level at higher energies.

$$T_{\mathrm{CH}} = T \int d\alpha \int d^2\vec{P}_{FT}\, n(\alpha, \vec{P}_{FT}) \frac{(\frac{d\sigma}{dt})_{pp}(s(\alpha))}{(\frac{d\sigma}{dt})_{pp}(s_0)}$$

$$\alpha \equiv A \frac{(E_F - P_{Fz})}{M_A} \simeq 1 - \frac{P_{Fz}}{m_p}$$

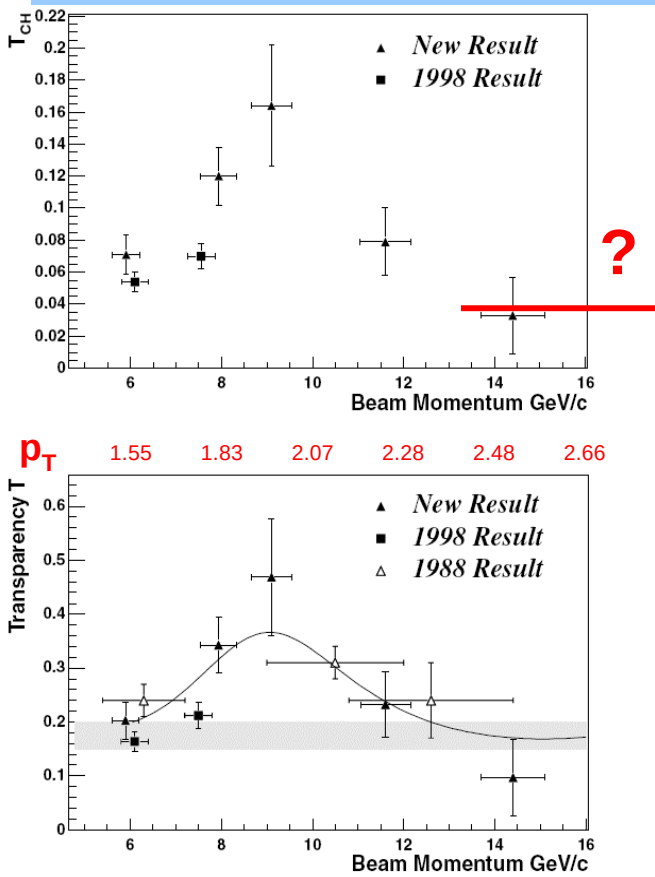

FIG. 2. Top: The transparency ratio T_{CH} as a function of the beam momentum for both the present result and two points from the 1998 publication [3]. Bottom: The transparency T versus beam momentum. The vertical errors shown here are all statistical errors, which dominate for these measurements. The horizontal errors reflect the α bin used. The shaded band represents the Glauber calculation for carbon [9]. The solid curve shows the shape R^{-1} as defined in the text. The 1998 data cover the c.m. angular region from 86°–90°. For the new data, a similar angular region is covered as is discussed in the text. The 1988 data cover 81°–90° c.m.

S.S.Shimanskiy

High p_T suppression in AA-collisions

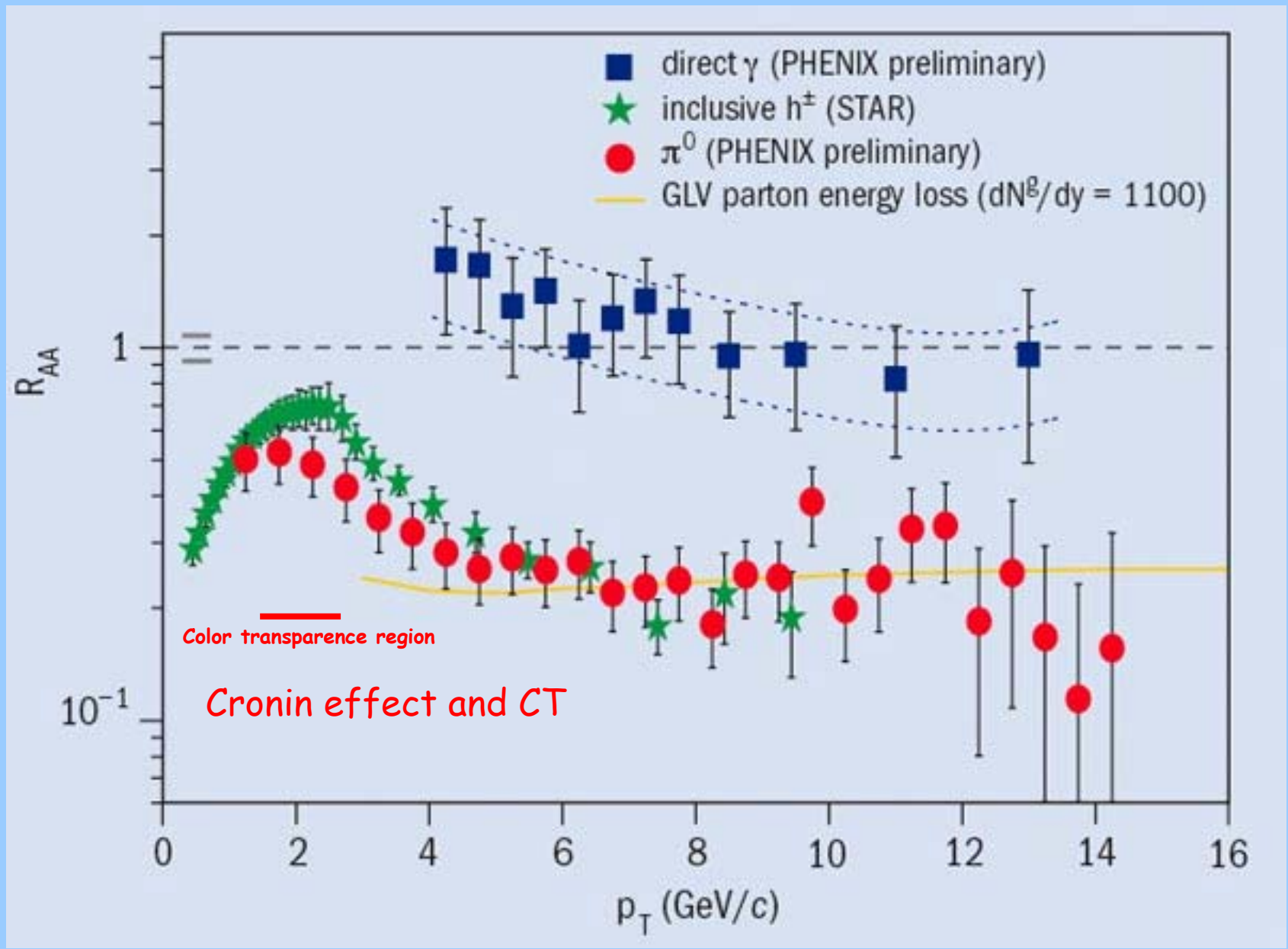

COLOR TRANSPARENCY

PHYSICAL REVIEW C **70**, 015208 (2004)

VIII. SUGGESTIONS FOR FUTURE EXPERIMENTS

Clearly there remain a number of interesting investigations involving nuclear transparency of protons and other hadrons. A revival of the AGS fixed target program [44], or the construction of the 50-GeV accelerator as part of the J-PARC complex in Japan [55], would provide excellent opportunities to expand the range of these nuclear transparency studies. Some of the remaining questions are the following.

(1) What happens at higher incident momentum? Does nuclear transparency rise again above 20 GeV/c, as predicted in the Ralston-Pire picture [56]?

(2) A-dependent studies in the 12 to 15 GeV/c range; will the effective absorption cross section continue to fall after the nuclear transparency stops rising at ~9.5 GeV/c [56]?

(3) At the higher energy ranges of these experiments the spin effects are expected to be greatly diminished. However, they continue to persist, as shown in both single and double spin measurements [34,57]. So it is important to see, in quasielastic scattering inside a nucleus, whether a relatively pure pQCD state is selected, and if the spin dependent effects are attenuated.

(4) Measurements of nuclear transparency with antiprotons, pions, and kaons will be informative. These particles have widely different cross sections at $90^{\circ}_{\text{c.m.}}$. For instance, the pp differential cross section at $90^{\circ}_{\text{c.m.}}$ is 50 times larger than the $\bar{p}p$ differential cross section [19]. How should this small size of the $\bar{p}p$ cross section affect the absorption of $\bar{p}$'s by annihilation?

(5) The production of exclusively produced resonances provides a large testing ground for nuclear transparency effects. This is especially true for those resonances that allow the determination of final state spin orientation, such as ρ's or Λ's [19,36]. Will the interference terms that generate asymmetries disappear for reactions which take place in the nucleus?

(6) Measurements in light nuclei that determine the probability of a second hard scatter after the first hard interaction are an alternative way to study nuclear transparency effects. With the proper kinematics selected, the probability of the second scatter is dependent on the state of the hadrons at the first hard interaction [58].

Cumulative(subthreshold) processes.

Fermi motion and SRC

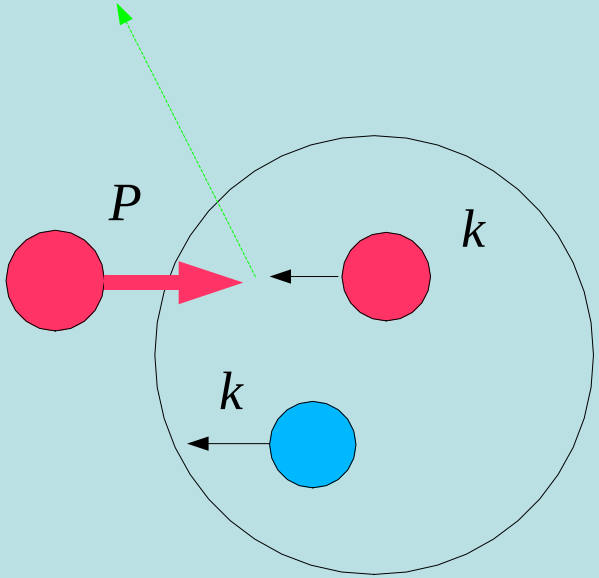

pA -> π, K, $\bar{p}$ ...+ X

$$\sigma_\pi \sim n(\vec{k}) \cdot \sigma(NN \to \pi, K + X)$$

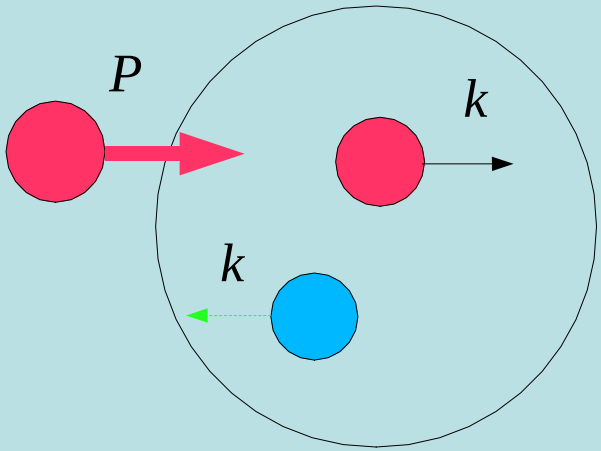

pA -> p,n + X

$$\sigma_N \sim n(\vec{k}) \cdot \sigma_0$$

Fluctons
(cumulative particle production)

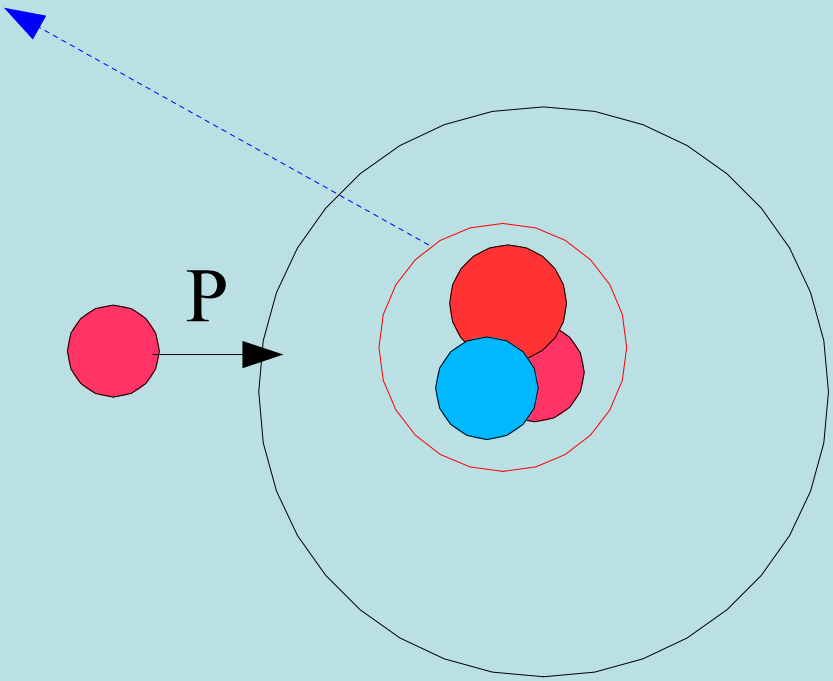

$$pA \to h + X$$

$$\sigma_h \sim P_K \cdot G_{h/K}(K)$$

Г.А.Лексин, ЯФ,т.65,2042(2002)

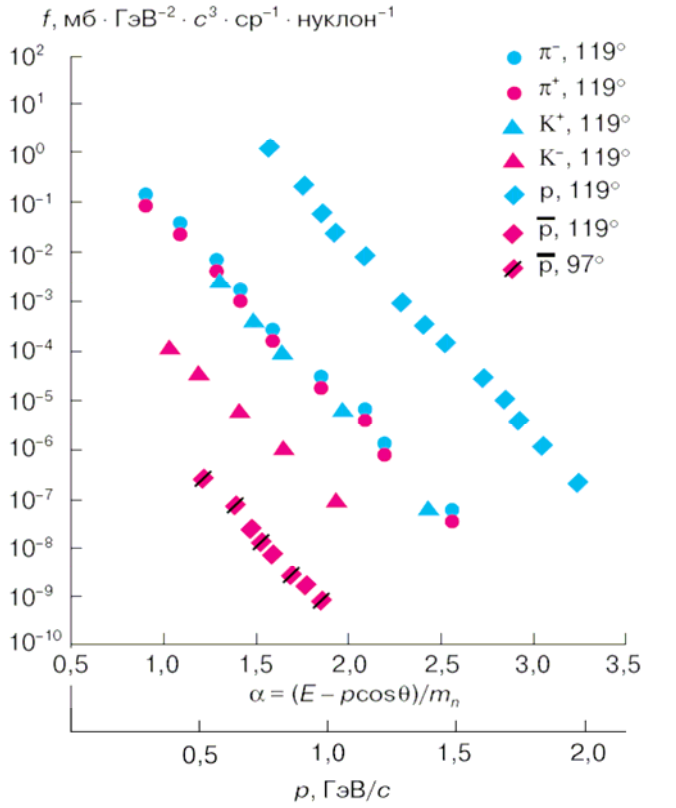

Рис. 2. Зависимость инвариантных функций различных кумулятивных частиц от их величин α. Нижняя шкала абсцисс – импульс кумулятивных протонов при соответствующем α.

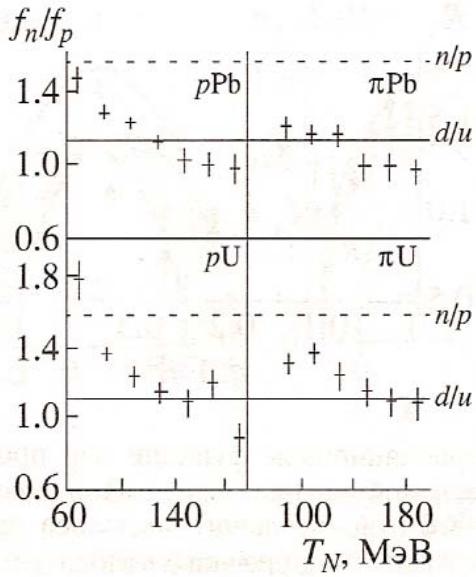

Рис. 12. Отношение выходов нейтронов к протонам из изонесимметричных ядер Pb и U в зависимости от кинетической энергии вылетающих нуклонов; угол вылета 120°, начальная энергия протонов 7.5 ГэВ и пионов 5 ГэВ. Данные, полученные под действием $\pi^{\pm}$-мезонов, усреднены. Штриховые линии — отношение нейтронов к протонам в ядрах мишени, сплошные — отношение d/u-кварков в ядрах Pb и U.

CURRENT EXPERIMENTS USING POLARIZED BEAMS OF THE JINR VBLHE ACCELERATOR COMPLEX

F. Lehar

DAPNIA, CEA/Saclay, Gif-sur-Yvette Cedex, France

Fiz. Elem. Chast. At. Yadra. 2005. V. 36. P. 954

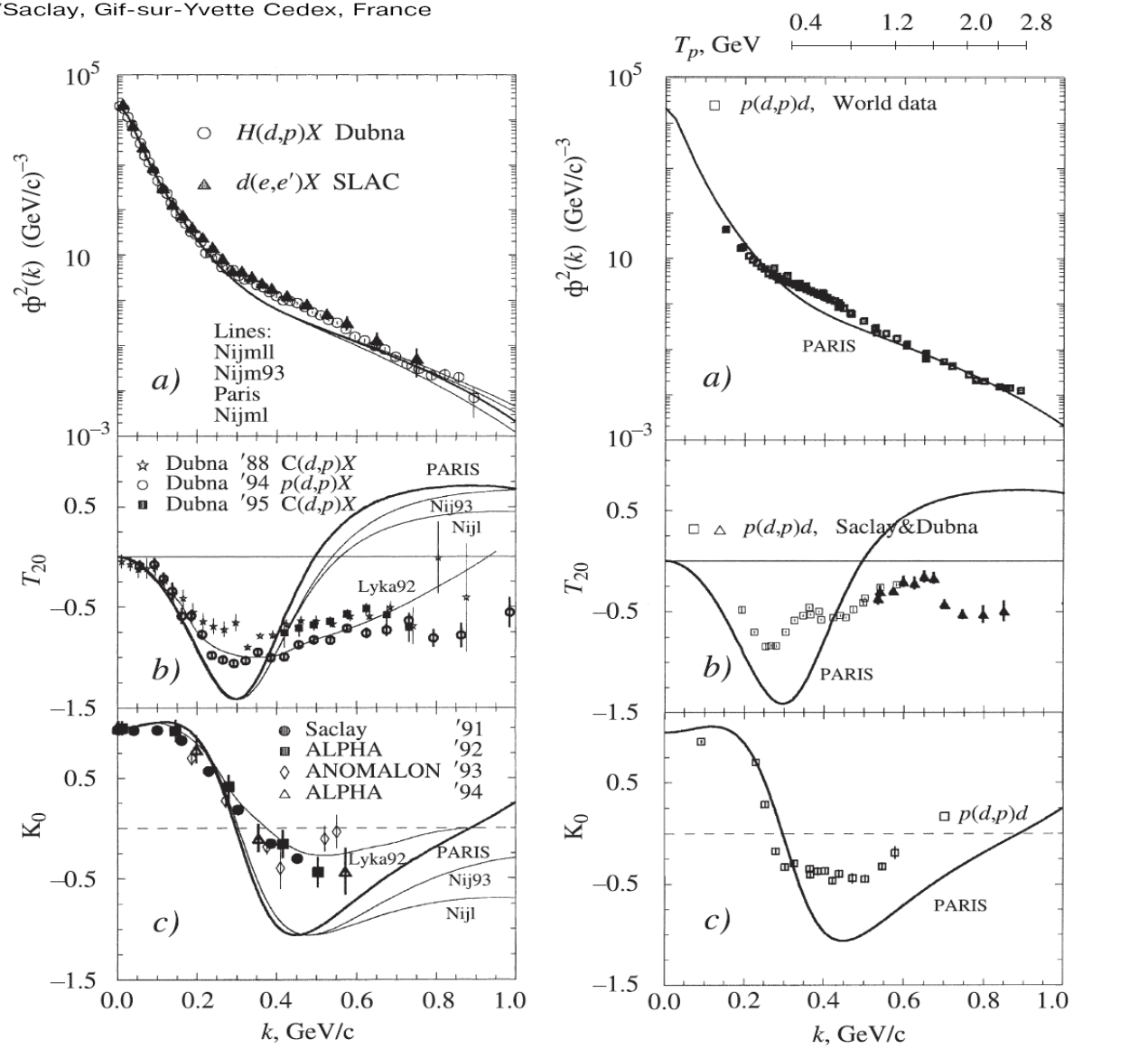

Рис. 5. Сводка данных экспериментов по фрагментации (слева) и упругому рассеянию «назад» (справа) поляризованных и неполяризованных дейтронов

The situation is very similar for cumulative(subthreshold) and high p_T processes there are very good description of cross sections(using constituent picture) and very bad understanding how to describe polarization.

"Counting rules" and the phenomenology give us direction for future physical investigations.

Huge polarization effects (high p_T pp-collisions and s.o.) give us additional tools.

CUMULATIVE(SUBTHRESHOLD) PROCESSES

Proceedings RNP 2005
S.S. nucl-ex/0604014

step which have open for us new way to resolve the cumulative puzzle. We need more complete investigation in the range of maximal p_T in semi-exclusive (and exclusive) experiment set up for comprehension of the nature of cumulative processes. It will need to investigate:

- average number of baryons accompanied high p_T cumulative particle production and its $s_{cumulat}$ dependance;

- average multiplicity accompanied high p_T cumulative particle production and its $s_{cumulat}$ dependance;

- $s_{cumulat}$ dependence of polarization characteristics (analyse power, asymmetry and so on), for SRC mechanism will be scaling repeating effects for free nucleon-nucleon interactions;

- coincidence cross sections of high p_T cumulative particle production with prediction of the "quark counting rules" [9] when using Stavinsky's variables.

With polarized ion beams we have real possibility to resolve many problems as are:

-"spin crisis"* of 70's ($p\uparrow p\uparrow, p\uparrow n\uparrow, n\uparrow n\uparrow$);

- color transparence ($p\uparrow A$, $p\uparrow {}^3He(d)\uparrow$);

-cumulative(subthreshold) particle production

...

*) next slide

"spin crisis" of 70's

A.D.Krish hep-ex/0511040

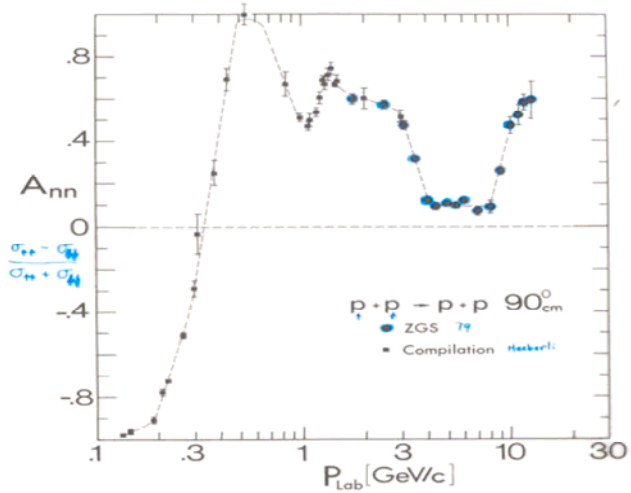

Figure 4: A_{nn} is plotted against P_{Lab}.

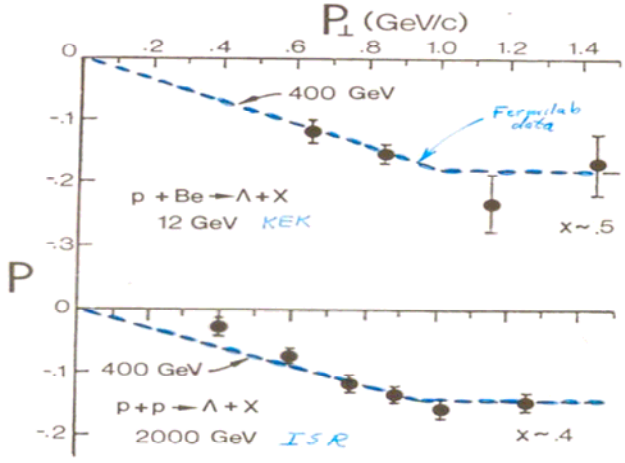

Figure 6: The Λ polarization is plotted against P_t^2.

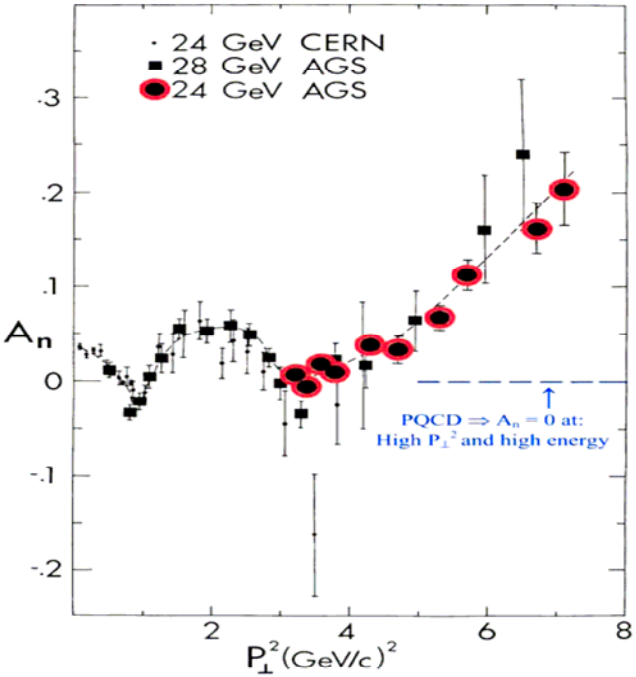

Figure 5: A_n is plotted against P_t^2.

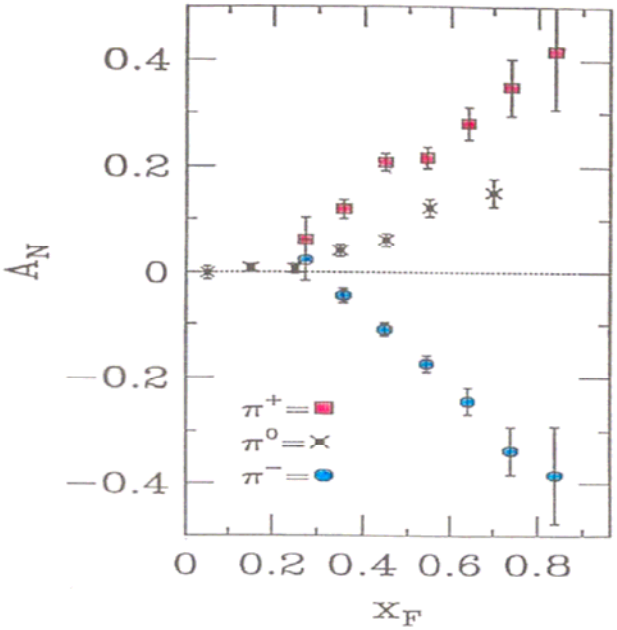

Figure 7: A_n is plotted against X_F for inclusive π-meson production.

Thank you for attention!